

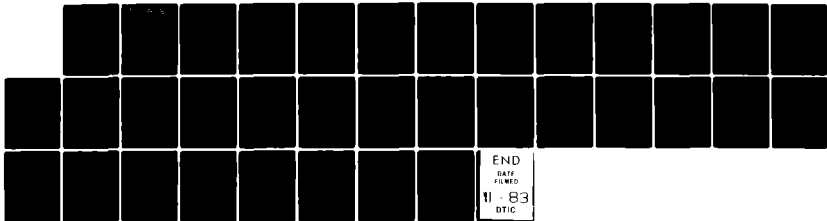
AD-A134 604

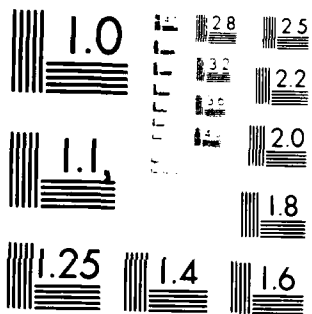
TEMPERATURE DEPENDENCE OF THE NO + O3 REACTION RATE
FROM 195 TO 369 K(U) NATIONAL AERONAUTICS AND SPACE
ADMINISTRATION GREENBELT MD GO. J V MICHAEL ET AL.
1982 FAA-EE-83-9 DTFA01-80-X-10559 F/G 4/1

1/1

UNCLASSIFIED

NL





MICROCOPY RESOLUTION TEST CHART
NATIONAL BUREAU OF STANDARDS-1963-A

(12)

Temperature Dependence of the NO + O₃ Reaction Rate from 195 to 369°K



U.S. Department
of Transportation
Federal Aviation
Administration

A134604

Office of Environment
and Energy
Washington, D.C. 20591

DTIC FILE COPY

DTIC
ELECTE
NOV 10 1983
S
A

This document has been approved
for public release and sale; its
distribution is unlimited.

J. V. Michael
J. E. Allen, Jr.
W. D. Brobst

FAA-EE-83-9

83 11 07 098

1. Report No. FAA-EE-83-9	2. Government Accession No. A134604	3. Recipient's Catalog No.	
4. Title and Subtitle Temperature Dependence of the NO + O ₃ Reaction Rate From 195 to 369°K		5. Report Date 1982	6. Performing Organization Code
7. Author(s) J.V. Michael*, J.E. Allen, Jr. and W.D. Brobst		8. Performing Organization Report No.	
9. Performing Organization Name and Address NASA Goddard Space Flight Center Laboratory for Planetary Atmospheres Greenbelt, Maryland 20771		10. Work Unit No. (TRAC)	11. Contractor Grant No. DTFA01-80-X-10559
12. Sponsoring Agency Name and Address U.S. Department of Transportation Federal Aviation Administration Office of Environment and Energy Air Quality Division Washington, D.C. 20591		13. Type of Report and Period Covered	
15. Supplementary Notes *Visiting Professor, Catholic University of America, Washington, D.C. Present Address: Brookhaven National Laboratory, Upton, New York.			
16. Abstract <p>The temperature dependence of the NO+O₃ reaction rate was examined using the fast flow technique. Several different experimental conditions and detection schemes were employed. With excess NO or excess O₃, NO₂ chemiluminescence was monitored. In addition, with excess O₃, NO was followed by fluorescence induced by an NO microwave discharge lamp. The results of the three independent sets of data are compared and found to agree within experimental error, indicating the absence of secondary chemistry which might complicate the kinetics. The data exhibit curvature on an Arrhenius plot; however, the simple Arrhenius expression $k = (2.6 \pm 0.8) \times 10^{-12} \exp(-1435 \pm 64/T) \text{cm}^3 \text{molecule}^{-1} \text{sec}^{-1}$ is an adequate description for $195 < T < 369^\circ\text{K}$. This result is compared to earlier determinations.</p>			
17. Key Words Ozone, Nitric Oxide, Reaction Rate, Temperature Dependence, Stratosphere, Chemiluminescence, Resonance Fluorescence		18. Distribution Statement Document is available to the public through the National Technical Information Service, Springfield, VA 22161	
19. Security Classif. of this report Unclassified	20. Security Classif. of this page Unclassified	21. No. of Pages 33	22. Price

Table Of Contents

Introduction	1
Experimental	2
Results	5
Discussion	9
Acknowledgements	15
References	16

List of Tables

I.	Rate Data for the Flow Discharge - Chemiluminescence Study of the Reaction $\text{NO} + \text{O}_3$; NO_2 Chemiluminescence, NO Excess.	19
II.	Rate Data for the Flow Discharge - Chemiluminescence Study of the Reaction $\text{NO} + \text{O}_3$; Chemiluminescence, O_3 Excess.	21
III.	Rate Data for the Flow Discharge-Reaction Fluorescence Study of the Reaction $\text{NO} + \text{O}_3$; NO Fluorescence, O_3 Excess.	24
IV.	Technique Independent Averaged Bimolecular Rate Constants for $\text{O}_3 + \text{NO}$.	26
V.	Arrhenius Expressions for the Temperature Dependent Data for Reaction (1).	27

List of Figures

1.	Temperature dependence of the NO_2 fluorescence intensity.	28
2.	Typical first order decay plots for NO_2 fluorescence technique; O_3 was the excess reagent.	29
3.	Diffusion corrected decay constants plotted vs. ozone concentration for experimental conditions of Fig. 2.	30
4.	Arrhenius plot for present data.	31



Introduction

Since the original observation of chemiluminescence by Greaves and Garvin,¹ the reaction



has received considerable attention. Interest has been sustained by the fact that the chemiluminescence arises from excited electronic states of nitrogen dioxide - $\text{NO}_2(^2\text{B}_2$ and/or $^2\text{B}_1$). Reaction (1) is therefore composite, since both ground state products, $\text{NO}_2(^2\text{A}_1)$, and excited state products, NO_2^* can result from a thermal distribution of reactant molecules. The exothermicity of reaction (1) to ground state products is $48 \text{ kcal mole}^{-1}$ which is ample energy to produce NO_2^* as well as $\text{O}_2(^1\Delta_g)$ at $22.6 \text{ kcal mole}^{-1}$ or $\text{O}_2(^1\Sigma_g^+)$ at $37.7 \text{ kcal mole}^{-1}$. There is no evidence that either excited state of O_2 is formed, however.

The first direct study covering an extended temperature range which addressed the question of the rate of reaction (1) was performed by Clyne, Thrush, and Wayne². These authors also examined the nature of the chemiluminescent emission in detail in order to identify the state of the emitting species. This work motivated over twenty additional studies which have addressed a variety of questions: rate enhancement by vibrational excitation of reactants, product states of NO_2 and O_2 , electronic state of NO and its effect on cross sections for the interaction, rotational effects on cross sections for the interaction, rotational effects for the interaction, and whether the interaction occurs through separate adiabatic potential energy surfaces or through nonadiabatic effects on a single potential energy surface. We need not review this state-to-state and predominately dynamical

work here since it has recently been thoroughly and thoughtfully reviewed by Chapman³ who concluded that: "A consistent interpretation of this diverse collection of information on the $O_3 + NO$ reaction is difficult."

In addition to this dynamical interest there has also been an interest in the thermal rate behavior. Reaction (1) occurs in a variety of complex reactive systems. Some of these systems are interesting for their illumination of fundamental chemical processes, while others attract attention for the roles they play in naturally occurring phenomena. Tropospheric and stratospheric chemistry are two systems in the latter category, and our specific motivation for the present work follows from the needs of tropospheric and stratospheric chemical modelers. Reaction (1) plays an important role in odd oxygen destruction in the NO_x cycle.

The data presented here were obtained by the fast flow technique. Two methods were utilized to follow the extent of reaction: nitrogen dioxide chemiluminescence and NO fluorescence induced by an NO microwave discharge lamp. The first technique parallels that of Clyne, Thrush, and Wayne²; however, data have been obtained with both NO and O_3 as the excess reagent. In the second technique O_3 is the excess reagent and the NO concentration is followed. This is the first such thermal study of this type on this system, and it is the first rate study to utilize induced NO fluorescence.

Experimental

The present experiments were performed using the flow technique with an apparatus which has been fully described previously.⁴ Only those modifications necessary for the present investigation will be described in detail.

Reaction (1) is relatively slow. As it was desirable to study the reaction with ozone as the excess reagent, the system was modified so that

large quantities of ozone could be prepared, purified, and stored. Ozone was generated by a commercial ozonizer and collected in a trap containing silica gel at -165°C . The trapped ozone was outgassed at liquid nitrogen temperature and subsequently transferred in pure liquid form to another liquid nitrogen cooled trap. The liquid sample was again thoroughly outgassed and was then vaporized into a light tight 12 l flask. Ozone was metered directly from the flask using a needle valve and was introduced either through the movable probe or into the bulk He flow.

Ozone concentrations were determined in situ by placing a photometer system diagonally across the flow tube downstream from the fluorescence/chemiluminescence detector. The photometer consisted of a low pressure mercury lamp as a source of 253.7 nm light, a 254 nm interference filter, and a 1P28 photomultiplier. Since the absorption coefficient - $308.5 \text{ cm}^{-1} \text{ atm}^{-1}$, base e, and 273°K - is known accurately, the direct determination of $[\text{O}_3]$ in the flow tube only depends on the measured transmittance and path length. This technique has been used in other studies from this laboratory.^{4c,5} At the flow conditions of the present study, there was a measurable Poiseuille pressure drop; consequently, corrections to flow velocities and $[\text{O}_3]$ were routinely made. Since the stored O_3 can slowly decompose to O_2 , it was necessary to develop a routine to assess the O_2 level in the stored sample and determine the bulk rate of decomposition. This was accomplished by accurately metering air into the system so as to reproduce the exact upstream and downstream pressures under the conditions of a given kinetic experiment. The $[\text{O}_3]$ was measured directly and all other flow rates were known; therefore, the O_2 mole fraction in the stored sample could be accurately determined. Considerable decomposition was noted with the newly constructed equipment. With continued use, however, the stored sample was remarkably stable, as high

as 85% ozone for periods of hours. New ozone samples were prepared daily. Some O_2 was always present in the sample; so, it was necessary to determine that no direct reaction occurred between NO and O_2 on the time scale of the present experiment. This was achieved by monitoring [NO] by induced fluorescence detection as a function of added [O_2]. No measurable reaction was observed. The other reagent, NO, was obtained from Scientific Gas Products and was purified by repeated bulb-to-bulb distillation at $-183^\circ C$ until the solid sample showed no trace of blue color. The concentration of NO was determined by accurately measuring the rate of pressure drop in a calibrated volume, as described previously.⁴ Other reagents were He (Airco, 99.9999%) as carrier gas, N_2O (Matheson, 98.0%) as the resonance lamp fill and O_2 (Matheson, 99.99%).

The chemiluminescence of excited NO_2 was measured with an R136 photomultiplier tube through a Corning glass 348 filter. In some O_3 excess experiments [NO] was determined by induced fluorescence. The NO discharge lamp contained 0.3 torr of pure continuously flowing N_2O and was excited by an electrodeless microwave (2450 MZ) discharge operating at a power of 20 watts. Spectral resolution of the subsequent NO emission was accomplished with an interference filter centered at 229.7 nm and having FWHM of 10.2 nm (Ed Barr Associates). This arrangement produced radiation which pumped the (0-0) γ band of the NO in the flow. A 1P28 photomultiplier detected the induced fluorescence through an interference filter centered at 248.6 nm with a FWHM of 12.5 nm (Ditric Optical). Therefore the (0-2) γ band in the flowing NO was primarily detected even though some (0-1) and (0-3) emission undoubtedly contributed. The Franck-Condon factor for (0-0) γ band absorption in NO is small,⁶ so that the sensitivity for NO detection with the present unoptimized fluorescence cell was not great. We determined in preliminary

experiments that the fluorescence signal was proportional to [NO] up to a concentration of $2 \times 10^{14} \text{ cm}^{-3}$. The reversal maximum was reached only when NO was nearly 1 torr ($2-3 \times 10^{16} \text{ cm}^{-3}$). A slight negative deviation from linearity became apparent between 2×10^{14} and $2 \times 10^{15} \text{ cm}^{-3}$. This behavior is three to four orders of magnitude less favorable than atomic fluorescence and is undoubtedly due to the low effective oscillator strength for (0-0) band absorption. The sensitivity, i.e., the concentration at a signal-to-noise ratio of one, was $3 \times 10^{11} \text{ cm}^{-3}$. Thus, concentrations of $2-3 \times 10^{13} \text{ cm}^{-3}$ were routinely utilized in the kinetic experiments. Higher sensitivity could undoubtedly be obtained with higher fluxes of exciting radiation, e.g., a laser at 226.9 nm and/or an optimized scattering cell with single photon detection capabilities. Neither point was pursued since no complications due to secondary reactions were expected in the present case.

Results

Since NO_2 chemiluminescence was selected as one of the methods for measuring the extent of reaction, it seemed appropriate to confirm the earlier results of Clyne, Thrush, and Wayne.² This exercise was motivated by the fact that to date their experiments have not been repeated even though their results appear to be uniformly lower than the value preferred for the rate constant.⁷ A question then arises concerning possible systematic error in the chemiluminescence detection technique. These authors rationalized the behavior of this chemiluminescence on the basis of the mechanism:





The emissive lifetime is known to be long compared to the quenching rates; that is, $\sum_1 k_{3i} [\text{M}_i] \gg k_2$. Under this condition and in the steady state, which is an appropriate approximation for the present flow velocities, the measured chemiluminescent intensity is

$$I = \frac{Ck_2 k_{1b} [\text{NO}] [\text{O}_3]}{\sum_1 k_{3i} [\text{M}_i]}, \quad (4)$$

where C is a system collection efficiency constant. For $k_2 = \tau_e^{-1}$ and k_{3i} considered to be temperature independent and one quencher - He in this case - dominating, the proportionality constant, $I_0 = Ck_2 k_{1b}/k_3^{\text{He}}$, will reflect the temperature dependence of the initial reaction channel (1b). Even though a minimal temperature dependence in quenching constants has been measured,⁸ the major dependence is due to reaction (1b).

The relation expressed in Eq. 4 was verified by measuring the chemiluminescent intensity at constant [NO] with varying [O₃] and vice versa. The [M]⁻¹ dependence was also tested and found to hold within the error of the present experiments. The Clyne, Thrush, and Wayne temperature dependence experiments on I₀ were repeated,² although the present data base is not as extensive as theirs. These results are shown in Fig. 1 where an exponential factor of $\exp(-2083 \pm 163/T)$ is indicated. Clyne, Thrush, and Wayne obtained $\exp(-2104 \pm 151/T)$,² and we therefore confirm both their rate law for emission as well as the temperature dependence for the path (1b).

Kinetic experiments were then performed with the flow technique under conditions which were similar to those of Clyne, Thrush, and Wayne;² that is, chemiluminescence was used to measure the extent of reaction with NO as the excess reagent. These results are shown in Table I.

In order to demonstrate the technique, specific kinetic results are illustrated for experiments for which O₃ was the excess reagent. Under these conditions [NO]_t is given by

$$\ln [\text{NO}]_t = -k_{1st} \frac{d}{v} + K, \quad (5)$$

where d is the distance from the variable probe tip to the detector, v is the linear flow velocity, and K is a constant. k_{1st} is the apparent first order decay constant and is related to the diffusion corrected first order decay constant by

$$k_{cor} = k_{1st} \left(1 + \frac{k_{1st} D}{v^2} \right). \quad (6)$$

D was calculated for diffusion in He by the Chapman-Enskog equation⁹ and corrections were made with Eq. 6 for the specific pressures and flow velocities for a given experiment. These corrections never exceeded 3%. k_{cor} is related to k₁, the bimolecular rate constant for reaction (1), by

$$k_{cor} = k_1 [O_3]_0. \quad (7)$$

Results obtained with this analysis scheme are shown in Fig. 2 where typical plots of ln [signal-background] against d expressed by Eq. 5 are given for one condition at 298°K. Note that via Eq. 4, [signal-background] is proportional

to $[NO]$ for constant $[O_3]$ and $[M]$. The apparent first order decay constants are diffusion corrected according to Eq. 6 and are then plotted against $[O_3]_0$ according to Eq. 7. Typical results are shown in Fig. 3.

The above analysis scheme was also used for the NO_2 chemiluminescent detection experiments with NO as the excess reagent. In this case $[O_3]$ was then followed, again via Eq. 4. These experiments, shown in Table I, correspond to the method utilized by Clyne, Thrush, and Wayne.² Their results give $k_1 = (0.97 \pm 0.20) \times 10^{-12} \exp(-1248 \pm 48/T) \text{ cm}^3 \text{ molecule}^{-1} \text{ s}^{-1}$ whereas those in Table 1 give $k_1 = (2.21 \pm 0.54) \times 10^{-12} \exp(-1391 \pm 55/T) \text{ cm}^3 \text{ molecule}^{-1} \text{ s}^{-1}$; both are expressed with 1σ errors. There is a significant difference in the results which appears to be outside of the combined experimental errors. We also note that definite curvature in the Arrhenius plot of the present result can also be seen.

Because of this discrepancy and the possibility of curved Arrhenius behavior, it was decided to study the reaction under excess O_3 conditions. Though none was expected, this procedure would test for any stoichiometric effect. The curved behavior could be the result of such a perturbation. These results are given in Table II. In addition data were obtained with the NO induced fluorescence technique under excess O_3 conditions. These experiments were performed to eliminate any artifact that might result from NO_2 chemiluminescence detection. These results are given in Table III.

Inspection of the three sets of results at the two standard deviation (95% confidence) level indicates no real systematic difference at any temperature. It should also be noted that at the 2σ level the intercepts from the plot of k_{COR} against $[reactant]$ are nearly always statistically indistinguishable from zero. Several points can be made: (a) NO_2 chemiluminescence is an excellent measurement of either $[NO]_t$ or $[O_3]_t$ with excess O_3 or NO , respec-

tively; that is, Eq. (4) holds rigorously. (b) There is no unexpected perturbation from secondary reactions. (c) Irrespective of the measurement technique the determinations at a given temperature can be averaged to obtain a technique independent value for $k(T)$. This is done in Table IV. (d) The grand average values of Table IV exhibit non-Arrhenius behavior as shown in Fig. 4. This point is also illustrated in Table IV by linear least squares analyses over different ranges of temperature.

Discussion

The rate data reported through 1976 on reaction (1) has already been thoroughly reviewed by Birks et al.,¹⁰ and it is this compilation that served as the basis for the NASA evaluation.⁷ There are a substantial number of room temperature determinations,¹¹⁻¹⁵ and the temperature dependence has been addressed in five additional studies.^{2,10,16-18} Since 1976 there have been two additional studies on the temperature dependence.^{19,20} The Arrhenius expressions for the temperature dependent data are listed in Table V along with the temperature range of each study. It should be noted that all of the previous studies were either carried out in the second order regime or with NO as the excess reagent. The present investigation represents the first study in which O₃ was the excess reagent.

Inspection of the results of Tables IV and V reveals some interesting points. The present results are indistinguishable from those of Johnston and Crosby,¹⁶ Huie et al.¹⁸ (as reported by Ray and Watson²⁰), and Lippmann et al.¹⁹ They are uniformly higher than those of Birks et al.¹⁰ and Ray and Watson²⁰ by ~10-15%. These latter two studies were performed with the same technique (DF-MS) and are in good agreement with one another. The present data do not agree with those of Clyne, Thrush, and Wayne² and Marte et al.¹⁷

We believe that much of the disagreement on this system is not random,

but instead is due to systematic differences. This can be illustrated with the present data by comparing it, for example, to that of Ray and Watson.²⁰ Over a similar range of temperatures, $230 < T < 369^\circ\text{K}$ compared to their $212 < T < 422^\circ\text{K}$, we obtain $k_1 = 3.6 \times 10^{-12} \exp(-1534/T) \text{cm}^3 \text{molecule}^{-1} \text{s}^{-1}$. Ray and Watson report $k_1 = 3.2 \times 10^{-12} \exp(-1556/T) \text{cm}^3 \text{molecule}^{-1} \text{s}^{-1}$. The exponential factors are identical within experimental error, but the present A factor is higher by $\sim 13\%$. Clearly such a situation could result from some minor systematic difference in the two apparatuses. A comparison with the results of Hule et al.¹⁸ over an even closer range of temperature ($224 < T < 364^\circ\text{K}$ instead of our $230 < T < 369^\circ\text{K}$), gives virtually exact agreement. Their result, as reported by Ray and Watson,²⁰ is $k_1 = 3.5 \times 10^{-12} \exp(-1533/T) \text{cm}^3 \text{molecule}^{-1} \text{s}^{-1}$.

In addition to systematic differences, the apparent disagreement in reported Arrhenius parameters also seems to be dependent on the range of temperatures over which a particular study was made. This is specifically seen in Table V and, for the present data, in Table IV and Fig. 4 where curved Arrhenius behavior is clearly indicated. It is this point which has created uncertainty for stratospheric modeling.⁷

The possibility of curvature in the Arrhenius plot was considered in the earlier work of Clyne, Thrush, and Wayne,² and it was documented and discussed by Birks et al.¹⁰ Clyne, Thrush, and Wayne,² and subsequently Clough and Thrush,²¹ determined the rate constant for reaction (1b) to be, $k_{1b} = (1.3 \pm 0.2) \times 10^{-12} \exp(-2104 \pm 151/T) \text{cm}^3 \text{molecule}^{-1} \text{s}^{-1}$, whereas that for reaction (1a) was $k_{1a} = 7.1 \times 10^{-13} \exp(-1173 \pm 75/T) \text{cm}^3 \text{molecule}^{-1} \text{s}^{-1}$. These values do not predict the extent of curvature found by Birks et al.¹⁰ who therefore suggested that $k_1 = k_{1a} + k_{1b} = 6.3 \times 10^{-13} \exp(-1200/T) + 7.1 \times 10^{-12} \exp(-2100/T) \text{cm}^3 \text{molecule}^{-1} \text{s}^{-1}$. This results in a ratio of A factors

(A_{1b}/A_{1a}) of 11.3, not 1.8 as determined by Clough and Thrush.²¹ If the present data are analyzed in precisely the same fashion as Birks et al.¹⁰ retaining their ratio of A factors, then k_1 is only slightly larger with $k_1 = k_{1a} + k_{1b} = 7.4 \times 10^{-13} \exp(-1200/T) + 8.2 \times 10^{-12} \exp(-2100/T) \text{ cm}^3 \text{ molecule}^{-1} \text{ s}^{-1}$. This expression is plotted in Fig. 4 where good agreement is seen with the present data. The expression can be empirically used for stratospheric modeling, yielding, for example, a value 15% higher at 230°K than currently recommended.⁷

The preceding analysis would, however, indicate that the process to form electronically excited NO_2 has an A factor which is over 10 times that for producing ground state products. Adoption of this scheme would suggest that channel (1b) accounts for about one third of the overall rate of 298°K. This disagrees with the results of Clough and Thrush²¹ who indicate only a 7% contribution at room temperature for that channel. Also reactions (1a) and (1b) would have equal rates of 374°K.

The question of the branching ratio has been an intriguing one for a number of years. Clough and Thrush,²¹ who determined that path (1b) accounted for 7% of the reaction at room temperature, also observed vibrational luminescence in the infrared. This long wavelength luminescence had the same T dependence as the electronic chemiluminescence from NO_2^* . They suggested that the vibrational emission arose from NO_2^* cascading into the upper levels of the NO_2 ground state. This point was questioned by Golde and Kaufman²² who confirmed the overall rate law for emission, but found the ratio of vibrational to electronic chemiluminescence to be 5.3 ± 1.0 . They argued that vibrationally excited NO_2 was predominantly formed in reaction (1a). The stationary target molecular beam experiments of Redpath et al.^{23,24} almost certainly confirm the Golde-Kaufman observation. Redpath et al. could also

rationalize their measured threshold energy (3.0 ± 0.6 kcal mole⁻¹) for production of NO₂* to that measured in the thermal reaction (4.2 kcal mole⁻¹ of Clyne, Thrush, and Wayne or 4.1 kcal mole⁻¹ in the present study) through a deconvolution procedure.

The crossed molecular beam experiments of Valentini, Cross, and Kwei²⁵ have also addressed the question of the branching ratio for reaction (1). With mass spectrometric detection of NO₂ products, these workers find distinct velocity and angular distribution differences for ground and excited NO₂ products. The ratio of NO₂ products is nearly constant and more or less independent of spin-orbit state or relative translational energy between 5 and 14 kcal mole⁻¹, even though an increase in cross section is observed over the same range of relative translational energy. They conclude that different potential energy surfaces probably exist for paths (1a) and (1b), but that curve crossings may occur. Also the near constancy of the ratio of NO₂ products is a direct measure of the ratio of cross sections for the two reactive paths at energies above threshold. Since the relative signals were more or less comparable, these results would suggest nearly equal preexponential factors for the thermal reaction. Therefore, their interpretation that more than one potential surface is involved and that paths (1a) and (1b) occur with similar frequency factors, agrees with the earlier conclusions of Clyne, Thrush, and Wayne² and Clough and Thrush.²¹

The necessity for two distinct channels was in fact indicated earlier in the molecular beam experiments of Redpath et al.^{23,24} who suggested that the differences were due to different reactivities of the two spin-orbit states of NO. Their assertion resulted from different behavior at different nozzle temperatures. This interpretation has not been confirmed in two other studies.^{25,26} Instead rotational enhancement is indicated. These workers²⁴

did show from state correlation arguments that ground state products were possible from end atom attack on O_3 by NO; however, formation of electronically excited NO_2 required the subsequent formation of electronically excited O_2 . This led them to suggest that excited NO_2 may result from central atom attack on O_3 by NO. This suggestion is by no means confirmed since Valentini, Cross, and Kwei²⁵ have assigned the ground state NO_2 product to the backscattered signal. They therefore suggest just the opposite, that central atom attack leads to ground state product while end atom attack leads to excited NO_2 .

The dynamical results on reaction (1) have not given a clear understanding to many of the details of the interaction. Two different potential energy surfaces are probable, perhaps involving two distinct intermediate configurations at the saddle points. This is the view taken by Chapman.³ Also, once the threshold barrier is overcome, the frequency for both paths is about the same.

The analysis given by Birks et al.¹⁰ leading to an A factor ratio for the two thermal rate constants of 11.8 would not appear to be in accord with the molecular beam results or results from measurements of absolute photon yields.^{2,21} It therefore seems probable that one or both of the thermal pathways, (1a) and (1b), may have significant T dependence in the preexponential factors. As shown earlier by Herschbach et al.²⁷ and Marte et al.,¹⁷ significant T dependence cannot be easily justified with activated complex theory. We have repeated the activated complex calculation for the A factor with one model that is quite similar to that of Marte et al.¹⁷

($\langle O_3 \rangle = 117^\circ$, $\langle ONO \rangle = 134^\circ$, and $\langle NO_2 \rangle = 125^\circ$; forming and breaking bond lengths are estimated from Pauling's rule with the assumption of one half bond order). With two free internal rotations, we obtain $A = (1.5 \times 10^{-11})$

$(1+\exp(-174/T))^{-1}T^{-1/2}q_v^\ddagger \text{ cm}^3\text{molecule}^{-1}\text{s}^{-1}$, where q_v^\ddagger is the vibrational partition function for the activated complex. This expression predicts an A factor of $(7 \times 10^{-13})q_v^\ddagger \text{ cm}^3\text{molecule}^{-1}\text{s}^{-1}$ for $195 < T < 260^\circ\text{K}$ and therefore, the prediction is within a factor of 1.6 of that indicated in Table IV over the same range of temperature. Inclusion of one low valued bending vibration ($150\text{--}200\text{cm}^{-1}$) would be sufficient to justify the result. However, the T dependence in A, $T^{-1/2}$, precludes this expression from being sufficient over the entire range of temperature. We point out that it is necessary to invoke two free rotations in the complex in order to come as close as indicated above. At higher T the observed A factor is higher than can be accommodated by any reasonable activated complex model. We have also made calculations on a middle atom attack complex: $\angle\text{ONO} = 134^\circ$, ONO plane perpendicular to O_3 plane, all $\angle\text{O}_3 = 60^\circ$, $r_{\text{ON}} = 1.2\text{\AA}$, $r_{\text{NO}} = 1.38\text{\AA}$ (in the O_3 plane), and all $r_{\text{O}_2} = 1.46\text{\AA}$. The result is $A = (2.6 \times 10^{-11})(1+\exp(-174/T))^{-1}T^{-1/2}q_v^\ddagger \text{ cm}^3\text{molecule}^{-1}\text{s}^{-1}$. This predicts values which are ~ 0.1 of those with the end on complex primarily because there can be only one free internal rotation for this model. We are led to conclude that activated complex theory cannot explain the extent of curvature found in the present study. One is therefore tempted to conclude that the curvature is entirely due to the two reactive pathways; however, this explanation, with the known T dependence of path (1b), really requires that A_{1b} be $\sim 10\text{--}20$ times higher than indicated experimentally^{21,25} or from activated complex theory. Also, inclusion of the second middle atom attack model makes the situation even more ambiguous from an activated complex point of view, since the predicted A factors would be even lower (~ 0.01 of that required).

The extensive work on the $\text{O}_3 + \text{NO}$ interaction notwithstanding, such fundamental questions as whether two potential surfaces are involved have not

been unambiguously answered. Redpath et al.²⁴ give several scenarios. Chapman³ has defined specific potential surfaces and has carried out trajectory calculations to facilitate understanding of the effect of reactant internal energy on the cross section. At this point the best that can be claimed is that this complex interaction is only partially understood.

ACKNOWLEDGEMENTS

We wish to thank Drs. L. J. Stief and J. J. Valentini for helpful discussions concerning the reaction and Dr. J. Margitan for discussions regarding the NO fluorescence. Support for this project by the FAA High Altitude Pollution Program under Interagency Agreement No. DTFA01-80-X-10559 is gratefully acknowledged.

Note: After completion of this work, recent results from a study by R. A. Borders and J. W. Birks were brought to our attention. Their data also suggest a curvature in an Arrhenius plot supporting our conclusions.

REFERENCES

1. J. C. Greaves and D. Garvin, *J. Chem. Phys.* 30, 348 (1959).
2. M.A.A. Clyne, B. A. Thrush, and R. P. Wayne, *Trans. Faraday Soc.* 60, 359 (1964).
3. S. Chapman, *J. Chem. Phys.* 74, 1001 (1981).
4. a) J. V. Michael and J. H. Lee, *Chem. Phys. Lett.* 51, 303 (1979).
b) J. H. Lee, J. V. Michael, W. A. Payne, and L. J. Stief, *J. Chem. Phys.* 69, 3069 (1978).
c) J. V. Michael and W. A. Payne, *Int. J. Chem. Kin.* 11, 799 (1979).
d) J. V. Michael, D. F. Nava, W. A. Payne, J. H. Lee, and L. J. Stief, *J. Phys. Chem.* 83, 2818 (1979).
5. a) J. V. Michael, J. H. Lee, W. A. Payne, and L. J. Stief, *J. Chem. Phys.* 68, 4093 (1978).
b) J. H. Lee, J. V. Michael, W. A. Payne, and L. J. Stief, *J. Chem. Phys.* 69, 350 (1978).
6. G. Herzberg, *Spectra of Diatomic Molecules*, Van Nostrand, New York, 1950.
7. NASA Reference Publication 1049, "The Stratosphere: Present and Future," R. D. Hudson and E. I. Reed, eds., 1979.
8. D. G. Keil, V. M. Donnelly, and F. Kaufman, *J. Chem. Phys.* 73, 1514 (1980).
9. J. O. Hirschfelder, C. F. Curtis, and R. B. Bird, *Molecular Theory of Gases and Liquids*, Wiley, New York, 1964.
10. J. W. Birks, B. Shoemaker, T. J. Leck, and D. M. Hinton, *J. Chem. Phys.* 65, 5181 (1976).
11. L. F. Phillips and H. I. Schiff, *J. Chem. Phys.* 36, 1509 (1962).

12. J. A. Ghormley, R. L. Ellsworth, and C. J. Hochanadel, *J. Phys. Chem.* 77, 1341 (1973); 78, 2698(E) (1974).
13. D. H. Stedman and H. Niki, *J. Phys. Chem.* 77, 2604 (1973).
14. P. P. Bemand, M.A.A. Clyne, and R. T. Watson, *J. Chem. Soc. Faraday Trans. 2* 70, 564 (1974).
15. K. H. Becker, U. Schurath, and H. Seitz, *Int. J. Chem. Kin.* 6, 725 (1974).
16. H. S. Johnston and H. J. Crosby, *J. Chem. Phys.* 22, 689 (1954).
17. J. E. Marte, E. Tschuikow-Roux, and H. W. Ford, *J. Chem. Phys.* 39, 3277, (1963).
18. "The Rate Constant for the Reaction $O_3 + NO \rightarrow O_2 + NO_2$ over the Temperature Range 224-364K," R. E. Huie, J. T. Herron, and R. L. Brown, 4th International Symposium on Gas Kinetics, Edinburgh, Scotland, August, 1975.
19. H. H. Lippmann, B. Jesser, and U. Schurath, *Int. J. Chem. Kin.* 12, 547 (1980).
20. G. W. Ray and R. T. Watson, *J. Phys. Chem.*, to be published.
21. P. N. Clough and B. A. Thrush, *Trans. Faraday Soc.* 63, 915 (1967).
22. M. F. Golde and F. Kaufman, *Chem. Phys. Lett.* 29, 480 (1974).
23. A. E. Redpath and M. Menzinger, *Can. J. Chem.* 49, 3063 (1971); *J. Chem. Phys.* 62, 1987 (1975).
24. A. E. Redpath, M. Menzinger, and T. Carrington, *Chem. Phys.* 27, 409 (1978).
25. J. J. Valentini, J. B. Cross, and G. H. Kwei (private communication).
26. S. L. Anderson, P. R. Brooks, J. D. Fite, and O. Van Nguyen, *J. Chem. Phys.* 72, 6521 (1980).

27. D. R. Herschbach, H. S. Johnston, K. S. Pitzer, and R. E. Powell, J.
Chem. Phys. 25, 736 (1956).

TABLE I: Rate Data for the Flow Discharge - Chemiluminescence Study of the Reaction $\text{NO} + \text{O}_3$; NO_2 Chemiluminescence, NO Excess.

$T, ^\circ\text{K}$	$P, \text{ torr}$	$v, \text{ cm s}^{-1}$	$[\text{NO}], 10^{-15}$ molecules cm^{-3}	$k_{\text{cor}}, \text{ a s}^{-1}$	slope ^b and intercept				
195	2.51	389	4.04	7.7+0.1	$S=(2.0\pm 0.2)\times 10^{-15}, \text{ a}$ $I=0.0\pm 1.6$				
			6.86	13.8+0.1					
			7.45	14.6+0.2					
			8.73	16.8+0.3					
			8.98	18.5+0.5					
			11.8	24.1+0.4					
			13.0	24.9+1.7					
	4.06	397	1.95	3.8+0.2	$S=(1.8\pm 0.1)\times 10^{-15}, \text{ a}$ $I=0.6\pm 0.4$				
			2.24	4.6+0.1					
			3.11	6.0+0.1					
			3.99	7.8+0.2					
			4.90	9.4+0.2					
			7.60	13.9+0.3					
			10.0	18.2+0.2					
			10.8	20.3+0.4					
			11.2	19.8+0.6					
			14.5	25.9+0.8					
			Results at 195°K, $k_1 = (1.9\pm 0.3)\times 10^{-15} \text{ a}$						
			230	2.67		406	1.40	6.9+0.2	$S=(5.0\pm 0.2)\times 10^{-15}, \text{ a}$ $I=-0.2\pm 1.5$
							1.90	9.9+0.3	
3.64	18.5+0.2								
4.49	21.6+0.3								
5.22	26.7+0.5								
5.64	27.5+0.5								
7.15	37.2+0.8								
8.64	43.0+0.6								
3.63	460	1.22		6.1+0.4	$S=(5.1\pm 0.6)\times 10^{-15}, \text{ a}$ $I=0.0\pm 2.9$				
		1.51		7.8+0.4					
		2.67		13.2+0.3					
		3.42		17.5+0.2					
		5.78		27.4+1.6					
		6.75		38.1+1.1					
		8.75		43.0+2.5					
		Results at 230°K, $k_1 = (5.1\pm 0.1)\times 10^{-15} \text{ a}$							
		260		2.41		567	1.14	11.4+0.2	$S=(9.7\pm 0.5)\times 10^{-15}, \text{ a}$ $I=1.2\pm 2.1$
							1.71	17.3+0.2	
							2.75	27.6+0.5	
							4.08	42.1+0.8	
4.75	49.0+0.7								
6.22	61.1+0.8								
6.97	67.2+0.9								

TABLE 1: Continued

T, °K	P, torr	ν , cm s ⁻¹	[NO], 10 ⁻¹⁵ molecules cm ⁻³	k_{cor} , a s ⁻¹	slope ^b and intercept			
	3.89	732	1.40	13.6±0.3	$S=(9.9\pm 0.4)\times 10^{-15}$, ^a $I=0.6\pm 1.3$			
			1.73	16.5±0.5				
			2.42	23.3±0.5				
			3.16	30.3±0.2				
			3.94	39.6±1.3				
			4.32	41.1±0.6				
			5.77	56.8±1.2				
			Results at 260°K, $k_1 = (9.8\pm 0.3)\times 10^{-15}$ a					
298	3.19	774	0.404	9.3±0.4	$S=(1.9\pm 0.1)\times 10^{-14}$, ^a $I=1.6\pm 1.8$			
			0.672	16.4±0.2				
			1.14	23.5±0.2				
			2.01	39.3±0.2				
			3.34	69.7±0.6				
			5.49	118.7±1.6				
			4.14	824		0.827	19.2±0.6	$S=(1.8\pm 0.1)\times 10^{-14}$, ^a $I=3.0\pm 3.1$
						1.77	39.4±0.8	
2.25	49.8±0.8							
2.80	63.0±2.2							
3.94	81.8±3.6							
5.92	126.0±1.8							
Results at 298°K, $k_1 = (1.9\pm 0.1)\times 10^{-14}$ a								
369	2.31	852			0.336	20.4±2.8	$S=(5.5\pm 0.9)\times 10^{-14}$, ^a $I=3.5\pm 8.2$	
			0.553	34.4±1.0				
			0.711	40.5±2.6				
			0.960	52.2±1.4				
			0.962	62.1±4.0				
			1.23	73.9±2.2				
			1.45	78.6±2.2				
	3.96	1022	0.598	34.5±1.0	$S=(6.0\pm 0.5)\times 10^{-14}$, ^a $I=4.3\pm 7.4$			
			0.814	42.9±0.8				
			1.11	63.9±4.2				
			1.43	76.3±1.2				
			1.75	99.3±1.8				
			2.24	132.8±1.6				
Results at 369°K, $k_1 = (5.7\pm 0.7)\times 10^{-14}$ a								

^aError limits are two standard deviations.

^bSlope, $S=k_1$, in units cm³ molecule⁻¹ s⁻¹.

TABLE II. Rate Data for the Flow Discharge-Chemiluminescence Study of the Reaction $\text{NO} + \text{O}_3$; NO_2 Chemiluminescence, O_3 Excess.

$T, ^\circ\text{K}$	$P, \text{ torr}$	$v, \text{ m s}^{-1}$	$[\text{O}_3], 10^{-15}$ molecules cm^{-3}	$k_{\text{cor}}, \text{ a s}^{-1}$	slope ^b and intercept				
195	2.47	391	1.45	3.3 ± 0.2	$S = (1.7 \pm 0.1) \times 10^{-15}, \text{ a}$ $I = 0.8 \pm 0.2$				
			2.00	4.4 ± 0.2					
			2.88	5.5 ± 0.3					
			3.63	6.9 ± 1.4					
			4.88	9.3 ± 0.4					
			6.55	11.8 ± 0.4					
			7.92	14.4 ± 0.3					
	3.77	389	1.75	3.9 ± 0.3	$S = (1.8 \pm 0.2) \times 10^{-15}, \text{ a}$ $I = 0.3 \pm 1.1$				
			3.18	5.7 ± 0.3					
			4.42	7.5 ± 0.3					
			5.21	9.1 ± 0.5					
			6.09	11.1 ± 0.6					
			7.34	12.7 ± 0.4					
			8.14	15.3 ± 0.9					
Results at 195°K , $\bar{k}_1 = (1.8 \pm 0.2) \times 10^{-15} \text{ a}$									
230	3.64	461	1.03	5.1 ± 0.5	$S = (4.6 \pm 0.7) \times 10^{-15}, \text{ a}$ $I = 1.0 \pm 1.6$				
			1.32	7.4 ± 0.7					
			2.13	11.4 ± 0.6					
			2.48	12.2 ± 0.3					
			2.97	14.2 ± 0.8					
	2.41	509	1.48	7.4 ± 0.4	$S = (4.7 \pm 0.3) \times 10^{-15}, \text{ a}$ $I = 1.1 \pm 1.3$				
			2.15	11.8 ± 0.6					
			2.98	14.5 ± 0.2					
			3.89	18.9 ± 0.7					
			4.94	25.1 ± 1.0					
			6.24	30.4 ± 0.4					
			7.23	34.0 ± 1.6					
			Results at 230°K , $\bar{k}_1 = (4.7 \pm 0.2) \times 10^{-15} \text{ a}$						
			260	2.35		578	1.14	10.6 ± 0.6	$S = (9.2 \pm 0.5) \times 10^{-15}, \text{ a}$ $I = 1.0 \pm 1.5$
1.53	15.1 ± 0.3								
1.91	19.3 ± 0.8								
2.37	22.6 ± 0.3								
2.86	28.5 ± 0.5								
3.74	34.7 ± 1.2								
4.56	42.7 ± 1.1								

TABLE II. Continued

T, °K	P, torr	v, cm s ⁻¹	[O ₃], 10 ⁻¹⁵ molecules cm ⁻³	k _{cor} , a s ⁻¹	slope ^b and intercept
	3.93	728	0.65 1.44 1.98 2.17 3.45 3.86	8.9+0.3 14.4+0.4 18.2+0.2 19.6+0.7 31.2+0.8 36.3+0.5	S=(8.5+0.8)x10 ⁻¹⁵ , ^a I=2.2+2.1
			Results at 260°K, k ₁ = (8.9+1.0)x10 ⁻¹⁵ a		
295	4.22	816	0.87 0.95 1.38 1.72 1.93 2.03 2.62 2.74 3.36 3.50 3.77 4.12 5.59	20.1+0.4 21.7+0.8 31.4+0.2 37.9+0.8 40.4+1.2 43.5+0.4 56.3+1.2 59.0+0.8 71.5+2.6 74.2+3.0 81.9+1.0 87.0+2.2 121.3+4.0	S=(2.1+0.1)x10 ⁻¹⁴ , ^a I=1.0+1.4
	4.28	735	1.41 1.84 2.30 3.15 4.19	29.7+0.3 40.3+0.2 52.0+0.7 65.5+0.4 87.2+0.5	S=(2.0+0.2)x10 ⁻¹⁴ , ^a I=2.9+4.8
	3.11	767	1.50 1.85 2.26 3.28 3.88	30.4+0.3 38.7+0.3 49.2+0.2 65.9+0.3 80.7+0.7	S=(2.0+0.2)x10 ⁻¹⁴ , ^a I=0.9+5.0
	2.15	672	1.53 2.09 2.63 3.15 3.83	32.8+0.3 43.0+0.6 55.7+0.5 66.8+0.4 83.0+0.6	S=(2.2+0.1)x10 ⁻¹⁴ , ^a I=-1.9+3.1
	1.46	581	1.71 2.24 2.73 3.24 3.99	36.2+0.1 46.3+0.3 56.0+0.3 70.8+0.5 86.2+0.4	S=(2.2+0.2)x10 ⁻¹⁴ , ^a I=-3.2+5.2
			Results at 298°K, k ₁ = (2.1+0.1)x10 ⁻¹⁴ a		

TABLE II. Continued

T, °K	P, torr	v, cm s ⁻¹	[O ₃], 10 ⁻¹⁵ molecules cm ⁻³	k _{cor} , ^a s ⁻¹	slope ^b and intercept
369	2.34	846	0.41	23.0+1.2	S=(5.3+0.5)x10 ⁻¹⁴ , ^a I=3.3+5.0
			0.63	38.2+1.2	
			0.92	52.9+2.0	
			1.25	72.0+2.8	
			1.63	88.0+2.8	
	3.96	1021	0.34	27.5+3.8	S=(5.5+0.7)x10 ⁻¹⁴ , ^a I=5.6+7.4
			0.44	30.6+1.8	
			0.70	40.2+1.8	
			0.98	61.5+1.0	
			1.25	68.4+1.8	
		1.79	107.7+2.2		
		2.39	124.3+3.8		
		Results at 369°K, k ₁ ⁻ = (5.4+0.3)x10 ⁻¹⁴ a			

^aError limits are two standard deviations.

^bSlope, S=k₁, in units cm³ molecule⁻¹ s⁻¹.

TABLE III: Rate Data for the Flow Discharge-Resonance Fluorescence Study of the Reaction $\text{NO} + \text{O}_3$; NO Fluorescence, O_3 Excess.

$T, ^\circ\text{K}$	$P, \text{ torr}$	$v, \text{ cm s}^{-1}$	$[\text{O}_3], 10^{-15}$ molecules cm^{-3}	$k_{\text{cor}}, \text{ a s}^{-1}$	slope ^b and intercept			
195	2.37	427	2.33	3.6 ± 0.2	$S = (1.8 \pm 0.5) \times 10^{-15}, \text{ a}$ $I = 0.5 \pm 0.1$			
			3.18	6.1 ± 0.5				
			4.41	8.4 ± 1.1				
			5.25	9.3 ± 0.6				
			6.68	11.0 ± 0.7				
			7.09	13.4 ± 1.0				
			4.16	467		2.46	4.2 ± 0.2	$S = (1.7 \pm 0.3) \times 10^{-15}, \text{ a}$ $I = 0.7 \pm 0.1$
	3.10	5.9 ± 0.5						
	4.01	8.1 ± 0.9						
	4.90	9.0 ± 0.9						
	5.61	10.8 ± 1.2						
	7.76	13.1 ± 1.5						
	Results at 195°K, $k_1 = (1.7 \pm 0.2) \times 10^{-15} \text{ a}$							
	230	2.18			558	1.12	5.9 ± 0.5	
			1.48	7.1 ± 0.5				
1.75			8.3 ± 0.7					
2.82			15.5 ± 0.9					
3.35			16.4 ± 0.8					
4.61			23.6 ± 0.6					
4.16			551	1.38		7.7 ± 0.7	$S = (4.6 \pm 0.5) \times 10^{-15}, \text{ a}$ $I = 1.7 \pm 1.0$	
		1.88		10.2 ± 0.8				
		2.31		12.0 ± 0.5				
		2.71		14.8 ± 0.6				
		2.85		15.3 ± 1.0				
		3.83		19.2 ± 1.0				
		4.59		22.5 ± 1.2				
		Results at 230°K, $k_1 = (4.9 \pm 0.8) \times 10^{-15} \text{ a}$						
260		2.67	542	1.19	11.6 ± 0.4	$S = (8.4 \pm 0.7) \times 10^{-15}, \text{ a}$ $I = 1.9 \pm 1.7$		
	1.66			16.4 ± 1.1				
	1.98			17.9 ± 0.5				
	2.25			20.5 ± 0.9				
	2.81			26.7 ± 1.0				
	3.33			29.7 ± 0.7				
	3.50			30.8 ± 1.5				
	4.13	643	0.784	8.7 ± 0.4	$S = (8.0 \pm 1.3) \times 10^{-15}, \text{ a}$ $I = 3.1 \pm 2.6$			
			1.04	10.1 ± 0.9				
			1.40	15.5 ± 0.8				
			1.89	19.1 ± 0.9				
			2.20	21.4 ± 0.7				
			2.55	24.9 ± 1.9				
			3.23	27.3 ± 2.0				
			Results at 260°K, $k_1 = (8.2 \pm 0.6) \times 10^{-15} \text{ a}$					

TABLE III (Continued)

	P , torr	v , cm s ⁻¹	$[O_3]$, 10 ⁻¹⁵ molecules cm ⁻³	k_{cor} , a s ⁻¹	slope ^b and intercept
325	2.20	710	0.590	11.9±1.2	$S=(2.2±0.4) \times 10^{-14}$, ^a $I=-0.9±7.8$
			1.04	20.9±1.2	
			1.57	30.1±1.4	
			2.10	49.2±5.4	
			2.82	53.7±6.0	
			3.49	78.8±6.0	
369	4.20	817	0.700	15.8±2.2	$S=(2.0±0.5) \times 10^{-14}$, ^a $I=1.9±7.4$
			1.06	19.8±0.8	
			1.21	27.5±3.0	
			1.83	39.1±1.6	
			2.54	59.9±3.0	
			2.88	56.5±9.6	
		3.09	60.8±4.8		
Results at 298°K, $k_1 = (2.1±0.5) \times 10^{-14}$ a					
369	2.29	785	0.215	13.2±0.8	$S=(6.6±1.1) \times 10^{-14}$, ^a $I=-2.7±6.0$
			0.307	19.2±0.8	
			0.477	26.1±0.6	
			0.581	32.3±2.0	
			0.670	41.5±1.4	
			0.867	57.3±4.8	
369	3.89	942	0.228	12.9±2.6	$S=(6.2±1.2) \times 10^{-14}$, ^a $I=0.1±7.8$
			0.326	19.3±1.4	
			0.332	21.8±0.6	
			0.525	32.3±2.4	
			0.662	49.8±2.2	
			0.814	50.0±2.0	
			0.834	45.6±9.8	
			0.981	62.8±4.8	
Results at 369°K, $k_1 = (6.4±0.6) \times 10^{-14}$ a					

^aError limits are two standard deviations.

^bSlope, $S=k_1$, in units cm³molecule⁻¹s⁻¹.

Table IV: Technique Independent Averaged Bimolecular Rate Constants
for $O_3 + NO$.

$\frac{T}{K}$	$k_1 \times 10^{14} \text{ }^{a,b}$
195	0.18 ± 0.02
230	0.49 ± 0.06
260	0.90 ± 0.15
298	2.0 ± 0.2
369	5.9 ± 1.0

Linear Least Squares Analyses:

$$369 \geq T \geq 195K: k_1 = (2.58 \pm 1.50) \times 10^{-12} \exp(-1435 \pm 128/T)^{a,b}$$

$$369 \geq T \geq 260K: k_1 = (5.23 \pm 0.48) \times 10^{-12} \exp(-1656 \pm 26/T)^{a,b}$$

$$260 \geq T \geq 195K: k_1 = (1.15 \pm 0.20) \times 10^{-12} \exp(-1258 \pm 38/T)^{a,b}$$

^a errors are two standard deviations

^b units are $\text{cm}^3 \text{ molecule}^{-1} \text{ s}^{-1}$

Table V: Arrhenius Expressions for the Temperature Dependent Data for Reaction (1).

$\frac{T}{K}$	$\frac{k_1}{\text{cm}^3 \text{ molecule}^{-1} \text{ s}^{-1}}$	<u>Reference</u>
198-230	$1.3 \times 10^{-12} \exp(-1250 \pm 150/T)$	16
216-322	$0.95 \times 10^{-12} \exp(-1230 \pm 75/T)$	2
245-345	$2.0 \times 10^{-12} \exp(-1275 \pm 110/T)$	17
203-361	$2.34 \times 10^{-12} \exp(-1450 \pm 50/T)$	10
224-364	$3.47 \times 10^{-12} \exp(-1533 \pm 64/T)^a$	18
283-443	$4.3 \times 10^{-12} \exp(-1598 \pm 50/T)$	19
212-422	$3.16 \times 10^{-12} \exp(-1556/T)$	20
195-369	$2.6 \times 10^{-12} \exp(-1435/T)$	this work

^aAs reanalyzed in Ref. 20.

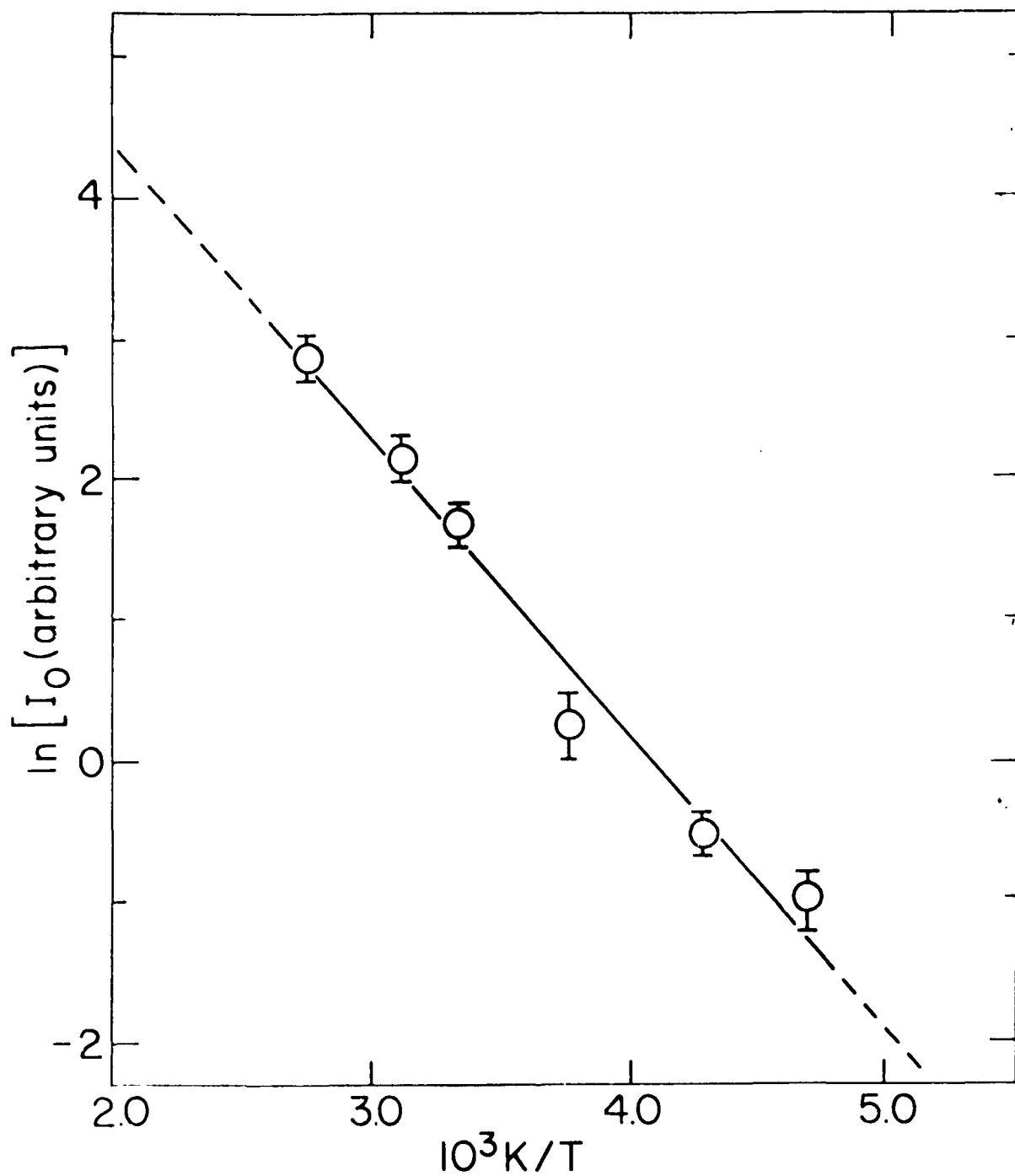


Figure 1. Temperature dependence of the NO_2 fluorescence intensity.

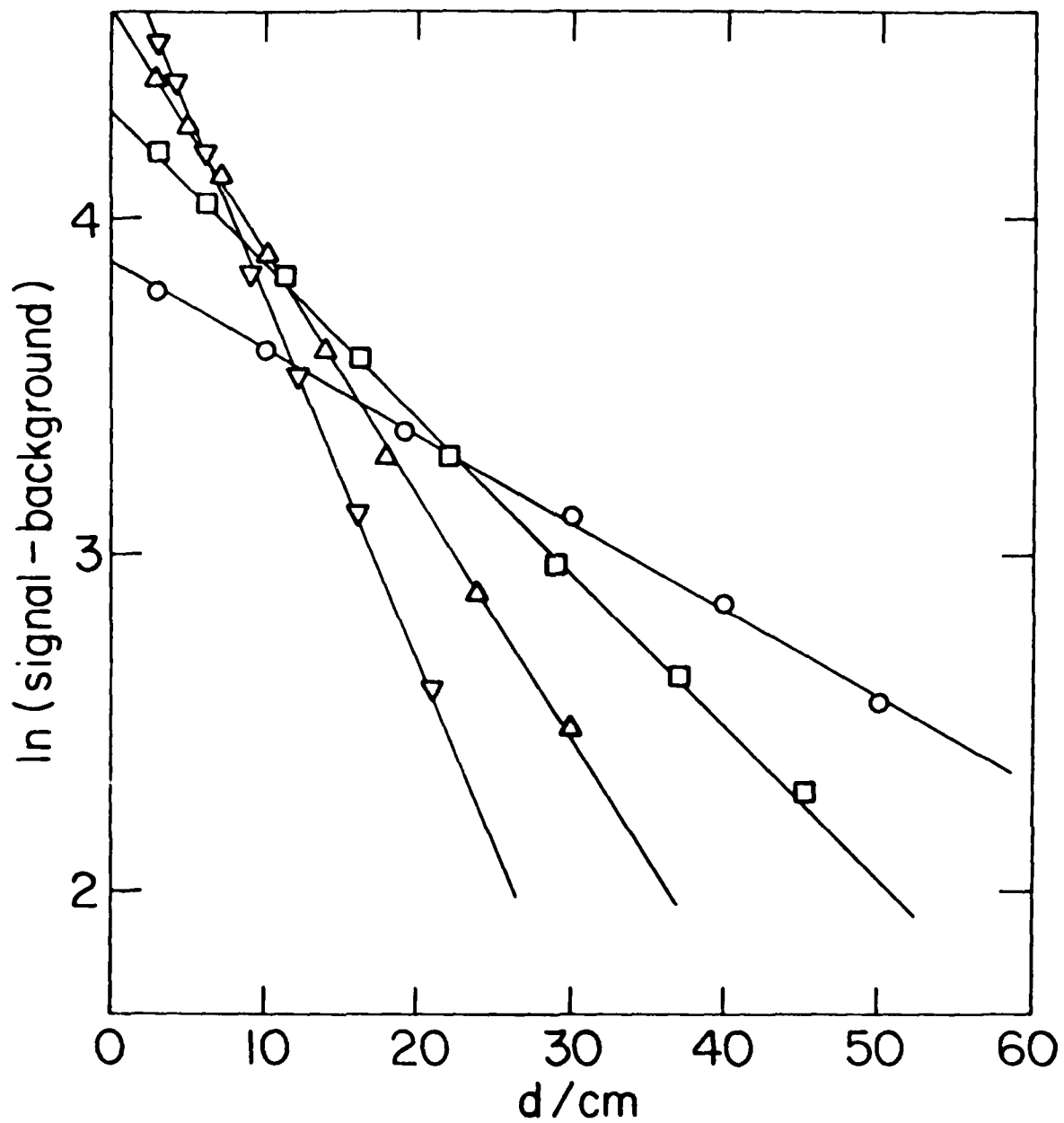


Figure 2. Typical first order decay plots for NO_2 fluorescence technique; O_3 was the excess reagent. Temperature, 298°K ; pressure 4.22 torr; flow velocity, 816 $\text{cm}\cdot\text{sec}^{-1}$; ozone concentration in 10^{-15} molecules- cm^{-3} : \circ -0.95, \square - 1.72, Δ -2.74, ∇ -4.12.

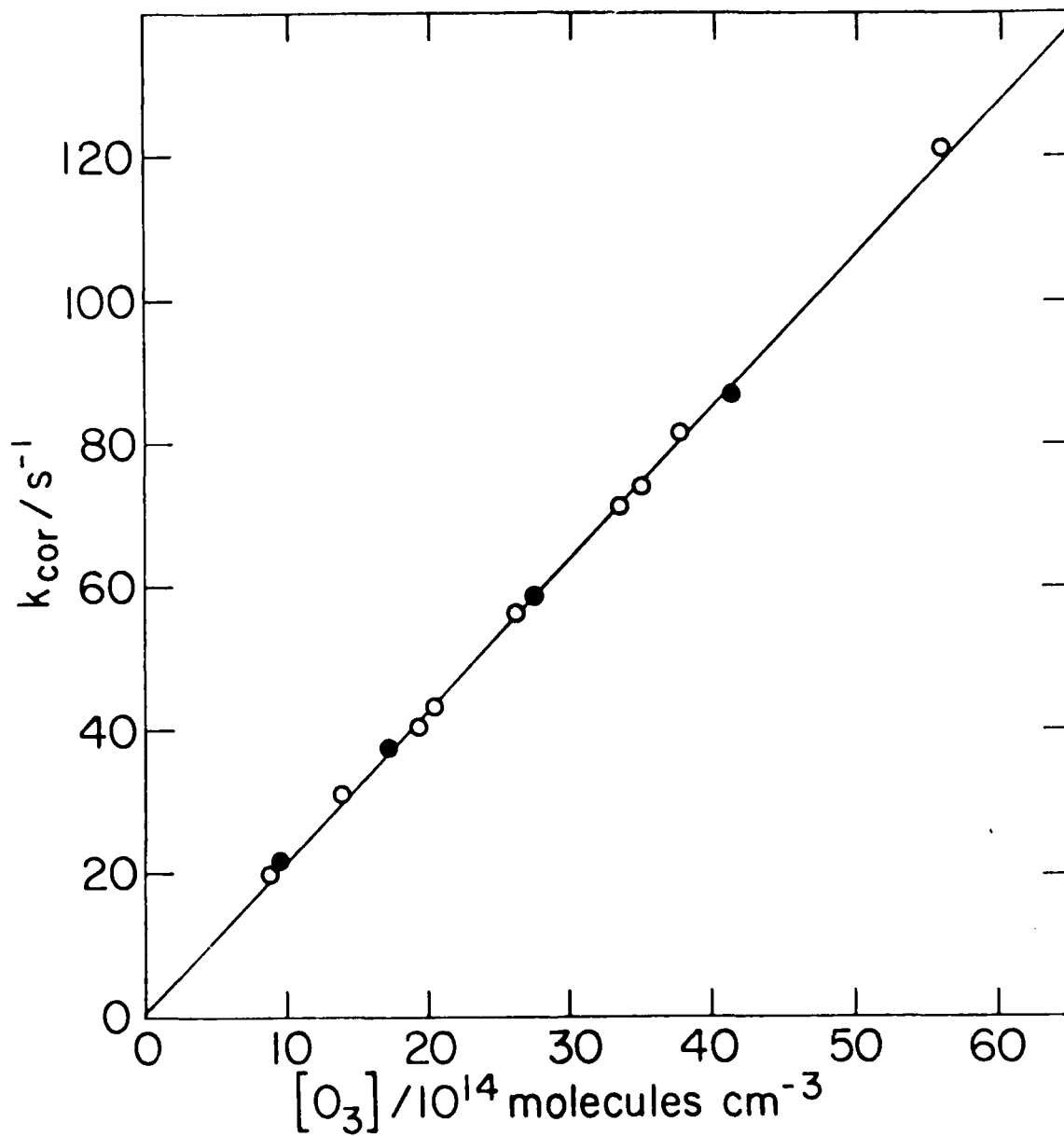


Figure 3. Diffusion corrected decay constants plotted vs. ozone concentration for experimental conditions of Fig. 2. The filled-in circles correspond to the apparent first order rates plotted in Fig. 2.

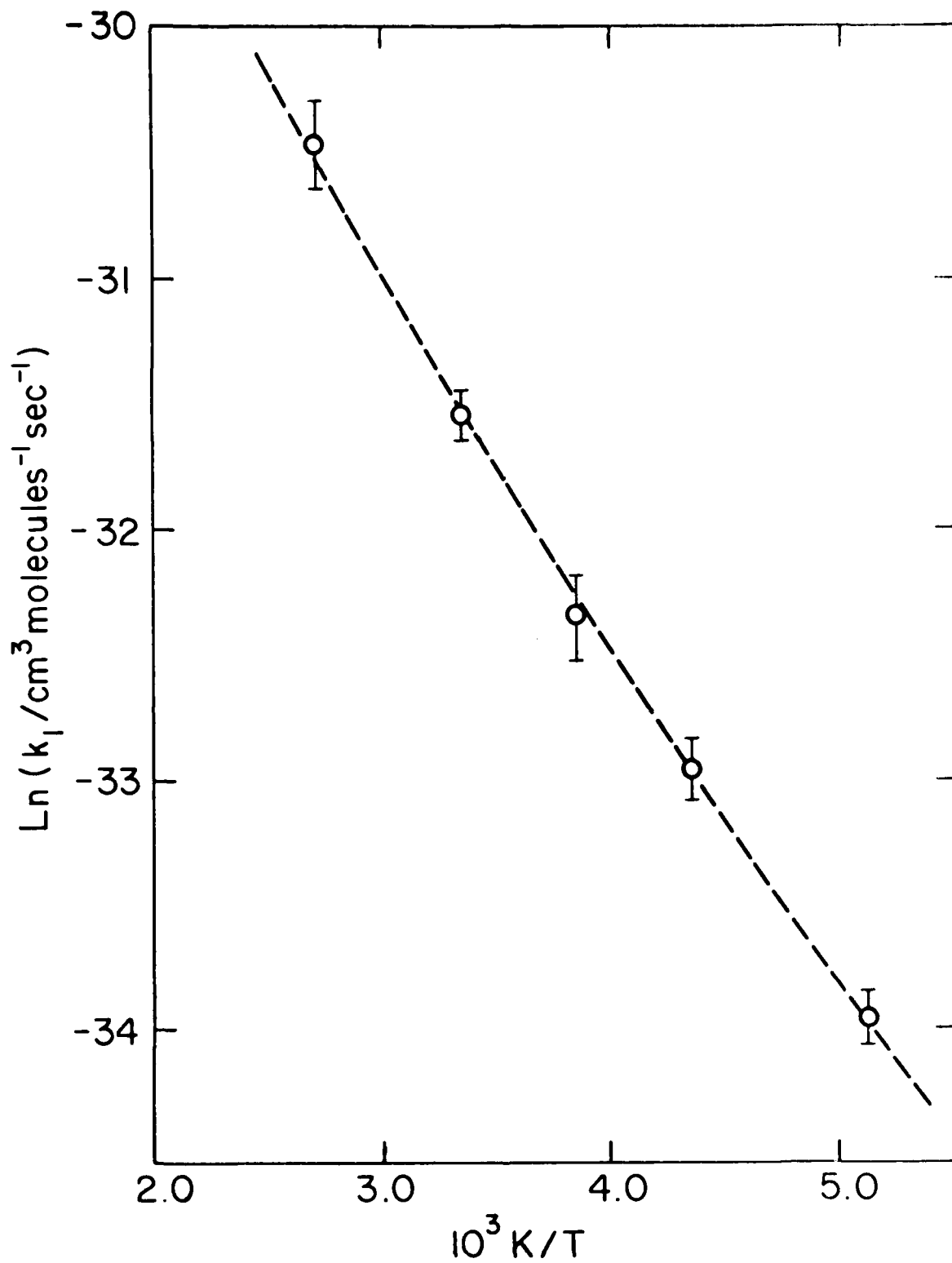


Figure 4. Arrhenius plot for present data. Dotted line is calculated (see text).

MED

8